Application of 3D Delaunay Triangulation in Fingerprint Authentication System

Wencheng Yang[1(✉)] , Guanglou Zheng[1], Ahmed Ibrahim[1],
Junaid Chaudhry[1], Song Wang[2], Jiankun Hu[3], and Craig Valli[1]

[1] Security Research Institute, School of Science, Edith Cowan University,
Perth, WA 6027, Australia
{w.yang, g.zheng, ahmed.ibrahim, j.chaudhry,
c.valli}@ecu.edu.au
[2] School of Engineering and Mathematical Sciences, La Trobe University,
Melbourne, VIC 3086, Australia
Song.Wang@latrobe.edu.au
[3] School of Engineering and Information Technology,
University of New South Wales at Canberra, Canberra, ACT 2600, Australia
J.Hu@adfa.edu.au

Abstract. Biometric security has found many applications in Internet of Things (IoT) security. Many mobile devices including smart phones have supplied fingerprint authentication function. However, the authentication performance in such restricted environment has been downgraded significantly. A number of methods based on Delaunay triangulation have been proposed for minutiae-based fingerprint matching, due to some favorable properties of the Delaunay triangulation under image distortion. However, all existing methods are based on 2D pattern, of which each unit, a Delaunay triangle, can only provide limited discrimination ability and could cause low matching performance. In this paper, we propose a 3D Delaunay triangulation based fingerprint authentication system as an improvement to improve the authentication performance without adding extra sensor data. Each unit in a 3D Delaunay triangulation is a Delaunay tetrahedron, which can provide higher discrimination than a Delaunay triangle. From the experimental results it is observed that the 3D Delaunay triangulation based fingerprint authentication system outperforms the 2D based system in terms of matching performance by using same feature representation, e.g., edge. Furthermore, some issues in applying 3D Delaunay triangulation in fingerprint authentication, have been discussed and solved. To the best of our knowledge, this is the first work in literature that deploys 3D Delaunay triangulation in fingerprint authentication research.

Keywords: 3D Delaunay triangulation · Fingerprint authentication

1 Introduction

The applications of fingerprint authentication can be found in both civil and military facets, e.g., Internet of Things (IoT), border control and financial transactions. As compared to other biometrics, such as face, voice, palm, ECG etc. [1–4], fingerprint

based authentication systems occupy the most market share because of the stability and distinctiveness that fingerprint can provide. However, fingerprint matching is not an easy task due to the fingerprint uncertainty caused by distortion, rotation and translation during the fingerprint image acquisition process. In order to mitigate the negative influence of fingerprint uncertainty, Delaunay triangulation based local structures have been proposed and studied by many existing methods, e.g., [5–8], for some specific local and global features that Delaunay triangulation can provide. First, each minutia in the Delaunay triangulation keep stable structure with its neighbors, despite a certain degree of non-linear distortion happens, which means that it has a stable local structure. Second, spurious and missing minutiae only influence the local units that contain those minutiae.

However, all existing methods in fingerprint authentication that include Delaunay triangulation are based on 2D pattern [9–14]. One drawback of using 2D Delaunay triangulation is that each unit, e.g., Delaunay triangle ΔABC, as shown in Fig. 1b, contains only a few features, three edges and three angles, which limit its distinctive capabilities and could lead to low system matching performance. Motivated by this, in this paper, we propose a 3D Delaunay triangulation based fingerprint authentication system. The main contribution of our work is two-fold: First, each unit in a 3D Delaunay triangulation (Fig. 2a) is a tetrahedron, e.g., ▲$ABCD$, as shown in Fig. 2b. Instead of three edges and three angles, each tetrahedron consists of six edges and twelve angles, which can provide higher distinctiveness than a triangle. Second, issues such as data normalization and local structure registration during the process of applying 3D Delaunay triangulation in the fingerprint authentication are discussed and solved.

2   2D and 3D Delaunay Triangulation Construction

In this section, we first introduce the 2D Delaunay triangulation construction. Given a fingerprint image which contains a set of minutiae $M = (m_1, m_2, m_3, \ldots, m_N)$, each minutia $m_{i \in [1,N]}$ can be represented by a vector $(x_i, y_i, \theta_i, t_i)$, where (x_i, y_i) is the Cartesian coordinate of the minutiae location, θ_i is the orientation of its associated ridge, and t_i is the minutia type. The generation of a 2D Delaunay triangulation only uses the coordinate (x_i, y_i) of each minutia and is based on the Voronoi tessellation which divides the whole fingerprint image into several smaller regions centering at each minutiae [15], as shown in Fig. 1a (red lines). By connecting the centers of every neighboring region, a 2D Delaunay triangulation is generated, as shown in Fig. 1b (blue lines). We have outlined the rationale for proposing the 3D Delaunay triangulation for the reason mentioned in the Introduction section. However, deployment of a 3D Delaunay triangulation in a fingerprint authentication system is not trivial, due to data normalization and local structure registration issues, thus need to be solved.

2.1   Data Normalization

During the generation of a 2D Delaunay triangulation, only two dimensions (x_i, y_i) of each minutia are needed, in contrast to three dimensions needed in a 3D Delaunay
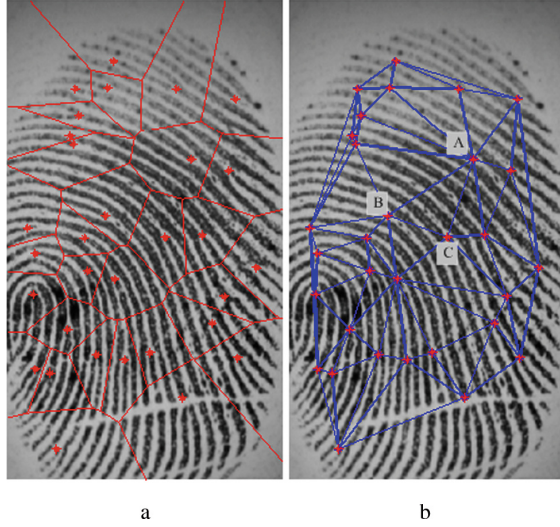
Fig. 1. (a) Minutiae-based Voronoi tessellation. (b) The 2D Delaunay triangulation with Delaunay triangle $\triangle ABC$ as an example. (Color figure online)

triangulation. In our application, θ_i is treated as the third dimension. For any minutia $m_{i \in [1,N]}$ extracted from a fingerprint image, its coordinate (x_i, y_i) are not on the same scale as the orientation θ_i. Take minutia $m_{i \in [1,N]}$ extracted by the commercial fingerprint recognition software Verifinger SDK [16] from fingerprint images of the public database FVC2002 DB2 [17] as an example. Its coordinate (x_i, y_i) is in the range of [0, 600] but its orientation θ_i is in the range of [0, 2 π]. To solve this issue, a normalization function is proposed as

$$N(\theta_i) = f_n(\theta_i, r_1[0, 2\pi], r_2[0, 600]) \qquad (1)$$

where $f_n(\cdot)$ is a normalization function that changes the value of θ_i from the range of [0, 2 π] to the range of [0, 600]; $r[x, y]$ represents the range between x and y. After the data normalization, a 3D Delaunay triangulation is generated, as shown in Fig. 2a.

2.2   Local Structure Registration

After the 3D Delaunay triangulation is constructed, one issue that needs to be solved before using the Delaunay tetrahedron for matching, is local structure registration. For example, there is a pair of corresponding Delaunay tetrahedrons, $\blacktriangle ABCD$ and $\blacktriangle A_1B_1C_1D_1$, from the template and query images, respectively. In this scenario, the correct local structure registration is about precisely finding out the corresponding vertexes of A, B, C and D from $\blacktriangle A_1B_1C_1D_1$. To simplify the issue of local structure registration, we use an absolute geometric measurement to decide which vertex is the top vertex. Specially, areas of four surfaces of a tetrahedron are calculated and the vertex opposite the largest surface is chosen as the top vertex. We assume that D is
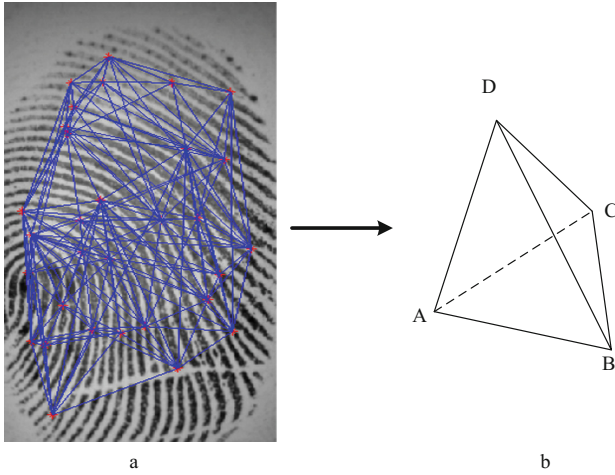
Fig. 2. (a) The 3D Delaunay triangulation. (b) A Delaunay tetrahedron ▲ABCD from the 3D Delaunay triangulation.

determined as the top vertex of ▲*ABCD*. Once the top vertex *D* is determined, the triangle Δ*ABC* is defined as the base. We then search the vertex of the smallest angle from Δ*ABC* and define it as the starting vertex *A* and the following vertexes as *B* and *C* in the anti-clockwise direction. By applying this measurement to the tetrahedron ▲$A_1B_1C_1D_1$, it is quite efficient to sort the vertexes A_1, B_1, C_1 and D_1, which are corresponding to vertexes of *A*, *B*, *C* and *D*, respectively. Note that if two surfaces have the same largest size, the top vertex can be chosen from either one of the two vertexes.

3   3D Delaunay Triangulation Based Fingerprint Authentication

Delaunay tetrahedron based local structure extracted from the 3D Delaunay triangulation is employed for authentication in this paper. Given a template fingerprint image f^T, the whole fingerprint image is divided into N^T local structures $\{L_i^T\}_{i=1}^{N^T}$, where N^T is the number of minutiae in f^T, and each local structure L_i^T is composed by all the Delaunay tetrahedrons constituted by a centre minutiae and its *K* nearest neighbor minutiae in the local area. Assuming that the ith local structure L_i^T contains $N_{L_i}^T$ Delaunay tetrahedrons, and all vertexes of each tetrahedron are sorted similar as ▲*ABCD* by the absolute geometric measurement. In the experiments, we only use the edge length as features for matching, so that the ith local structure L_i^T can be represented by

$$L_i^T = \left\{ eAB_j, eBC_j, eCA_j, eDA_j, eDB_j, eDC_j \right\}_{j=1}^{N_{L_i}^T} \tag{2}$$

where eAB is the quantized edge length between the vertexes A and B using the same way in [14], and the quantization step size is q_e. Then the template fingerprint image f^T is expressed as a feature set $V^T = \{L_i^T\}_{i=1}^{N^T}$, which is stored in the database as a template in the enrolment stage. In the verification stage, given a query fingerprint image f^Q, we apply the same feature extraction and representation approach to it and obtain a feature set $V^Q = \{L_j^Q\}_{j=1}^{N^Q}$, where N^Q is the number of minutiae from f^Q. The matching score between L_i^T and L_j^Q depends on how many Delaunay tetrahedrons are matched. Two tetrahedrons are considered to be a match, if and only if all the six quantized edge lengths of two tetrahedrons are the same. Assuming the number of matched tetrahedron between L_i^T and L_j^Q are N_{ij}, the similarity score between them is calculated by

$$S(ij) = \frac{N_{ij}}{(N_{L_i}^T + N_{L_j}^Q)/2} \tag{3}$$

Each L_j^Q from the query, for $1 \leq j \leq N^Q$, has to be compared with each L_i^T from the template, for $1 \leq i \leq N^T$. By comparing all the local structures from template and query, a score matrix of size $N^Q \times N^T$ is generated. If the largest value S_m from the score matrix is greater than a pre-defined threshold, the template and the query fingerprint images are considered a match.

4   Experimental Results and Analysis

We evaluated the proposed fingerprint authentication system over the public database FVC2002 DB2 [17], which includes 100 fingers with eight images per finger. The commercial fingerprint recognition software Verifinger SDK [16] is employed to extract minutiae from fingerprint images. The indicators, Equal Error Rate (EER), False Rejection Rate (FRR) and False Acceptance Rate (FAR), are adopted in our experiments to evaluate the system performance. Specifically, FRR is the rate of mistaking two fingerprint images from the same finger to be from two different fingers. The FAR is the rate of mistaking two different fingers to be from the same finger. The EER is the error rate when FRR and FAR are equal. We used the first image from each finger as the template and the second image from the same finger as the query image to calculate FRR, while we set the first image of each finger as template and the first image from all other different fingers as query image to calculate FAR.

To facilitate the comparison of the system matching performance, we only used the edge length of each unit as features to evaluate the matching performance in both 2D and 3D Delaunay triangulation based experiments. It is worth mentioning that other features, e.g., angle and minutia type, can be added to enhance the matching performance. Other parameters are set to be the same, for example, the quantization size q_e is set to be 20 and the value of K is 10 for both experiments. The performances of the system using the 2D and 3D Delaunay triangulation, respectively, are shown in Fig. 3, from which we can see that the performance of system using 3D Delaunay triangulation is EER = 7%, which is much better than the performance (EER = 6.37%) of system

using 2D Delaunay triangulation. This improved performance verifies that each unit, a Delaunay tetrahedron, from a 3D Delaunay triangulation can provide higher discrimination ability than the unit, a Delaunay triangle, from a 2D Delaunay triangulation.
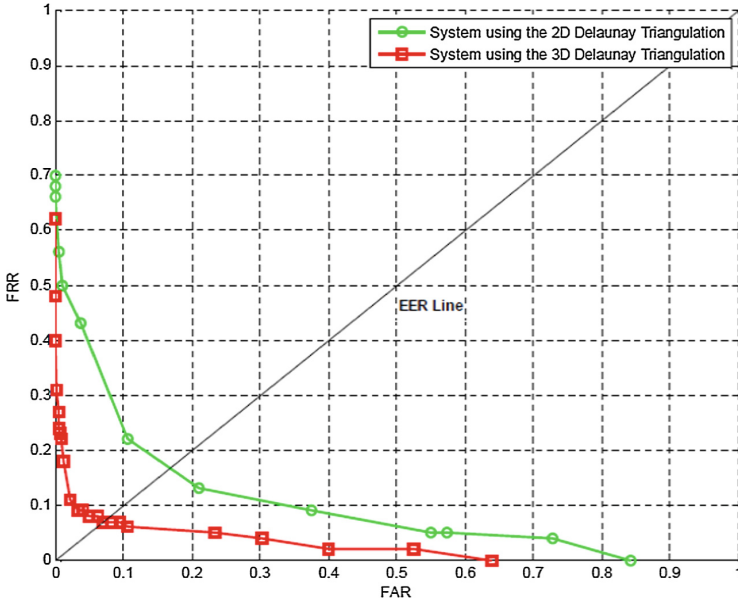

Fig. 3. The performances of system using 2D Delaunay triangulation and 3D Delaunay triangulation, respectively.

5   Conclusion

In this paper, we applied a 3D Delaunay triangulation in fingerprint authentication rather than a 2D Delaunay triangulation utilized by existing work in the literature, so as to increase the discrimination ability of each unit in a Delaunay triangulation. Experimental results show that each unit from a 3D Delaunay triangulation is more distinctive than a single unit from a 2D Delaunay triangulation. Moreover, certain issues, e.g., data normalization and local structure registration, anticipated in the process of applying the 3D Delaunay triangulation in the fingerprint authentication system were discussed and solved. This is the first work applying 3D Delaunay triangulation in fingerprint authentication and we hope that this work would be a useful starting point for future research, e.g., in the area of cancelable biometrics [18–23].

References

1. Zheng, G., Fang, G., Shankaran, R., Orgun, M.A.: Encryption for implantable medical devices using modified one-time pads. IEEE Access **3**, 825–836 (2015)
2. Fang, G., Orgun, M.A., Shankaran, R., Dutkiewicz, E., Zheng, G.: Truthful channel sharing for self coexistence of overlapping medical body area networks. PLoS ONE **11**, e0148376 (2016)
3. Zheng, G., Shankaran, R., Orgun, M.A., Qiao, L., Saleem, K.: Ideas and challenges for securing wireless implantable medical devices: a review. IEEE Sens. J. **17**, 562–576 (2016)
4. Zheng, G., Fang, G., Shankaran, R., Orgun, M.A., Zhou, J., Qiao, L., Saleem, K.: Multiple ECG fiducial points-based random binary sequence generation for securing wireless body area networks. IEEE J. Biomed. Health Inform. **21**, 655–663 (2017)
5. Bebis, G., Deaconu, T., Georgiopoulos, M.: Fingerprint identification using Delaunay triangulation. In: International Conference on Information Intelligence and Systems, pp. 452–459 (1999)
6. Liu, N., Yin, Y., Zhang, H.: A fingerprint matching algorithm based on Delaunay triangulation net. In: The 5th International Conference on Computer and Information Technology, pp. 591–595. IEEE (2005)
7. Wang, C., Gavrilova, M.L.: Delaunay triangulation algorithm for fingerprint matching. In: 3rd International Symposium on Voronoi Diagrams in Science and Engineering, pp. 208–216 (2006)
8. Yang, W., Hu, J., Wang, S., Stojmenovic, M.: An alignment-free fingerprint bio-cryptosystem based on modified Voronoi neighbor structures. Pattern Recogn. **47**, 1309–1320 (2014)
9. Junior, P., de Nazare-Junior, A., Menotti, D.: A complete system for fingerprint authentication using Delaunay triangulation. Re-conhecimento de Padroes, DECOM UFOP, pp. 1–7 (2010)
10. Yang, W., Hu, J., Stojmenovic, M.: NDTC: a novel topology-based fingerprint matching algorithm using N-layer Delaunay triangulation net check. In: 2012 7th IEEE Conference on Industrial Electronics and Applications (ICIEA), pp. 866–870. IEEE (2012)
11. Yang, W., Hu, J., Wang, S.: A Delaunay triangle-based fuzzy extractor for fingerprint authentication. In: 2012 IEEE 11th International Conference on Trust, Security and Privacy in Computing and Communications (TrustCom), pp. 66–70. IEEE (2012)
12. Yang, W., Hu, J., Wang, S.: A Delaunay triangle group based fuzzy vault with cancellability. In: 2013 6th International Congress on Image and Signal Processing (CISP), pp. 1676–1681 (2013)
13. Yang, W., Hu, J., Wang, S., Yang, J.: Cancelable fingerprint templates with Delaunay triangle-based local structures. In: Wang, G., Ray, I., Feng, D., Rajarajan, M. (eds.) CSS 2013. LNCS, vol. 8300, pp. 81–91. Springer, Cham (2013). https://doi.org/10.1007/978-3-319-03584-0_7
14. Yang, W., Hu, J., Wang, S., Chen, C.: Mutual dependency of features in multimodal biometric systems. Electron. Lett. **51**, 234–235 (2015)
15. Lee, D.-T., Schachter, B.J.: Two algorithms for constructing a Delaunay triangulation. Int. J. Comput. Inf. Sci. **9**, 219–242 (1980)
16. VeriFinger SDK: Neuro Technology. <http://www.neurotechnology.com/verifinger.html>
17. http://bias.csr.unibo.it/fvc2002
18. Wang, S., Hu, J.: A blind system identification approach to cancelable fingerprint templates. Pattern Recogn. **54**, 14–22 (2016)
19. Wang, S., Hu, J.: Design of alignment-free cancelable fingerprint templates via curtailed circular convolution. Pattern Recogn. **47**, 1321–1329 (2014)

20. Wang, S., Hu, J.: Blind channel estimation for single-input multiple-output OFDM systems: zero padding based or cyclic prefix based? Wirel. Commun. Mob. Comput. **13**, 204–210 (2013)
21. Wang, S., Hu, J.: Alignment-free cancellable fingerprint template design: a densely infinite-to-one mapping (DITOM) approach. Pattern Recogn. **45**, 4129–4137 (2012)
22. Wang, S., Deng, G., Hu, J.: A partial Hadamard transform approach to the design of cancelable fingerprint templates containing binary biometric representations. Pattern Recogn. **61**, 447–458 (2017)
23. Wang, S., Yang, W., Hu, J.: Design of alignment-free cancelable fingerprint templates with Zoned Minutia Pairs. Pattern Recogn. **66**, 295–301 (2017)